

Three Dimensional Inversion of SWARM Satellite Magnetic Data

Pascal Tarits

IUEM, Place Nicolas Copernic, F29280 Plouzané, France

email: tarits@univ-brest.fr

INTRODUCTION

The purpose of the study presented in this report is to demonstrate the feasibility of 3-D conductivity inversion using satellite magnetic data. With the forthcoming of the Swarm constellation project for magnetic studies, a new era for global induction studies is opening with new ways to infer the electrical conductivity in the earth.

The situation is very unusual for induction studies as the transient magnetic field is sampled simultaneously both in time and space. It is however sampled at a high rate and continuously over the earth. Several studies have demonstrated the feasibility of induction studies from space for simple source geometries and one dimensional (1-D) conductivity models (e.g. [1]). The main objective of space induction is to obtain data to image the 3-D mantle conductivity. Studies to date suggest that a 3-D induction signal is present in the satellite data [2, 3]. Here, a full solution to this problem is tested. The first step consists of data processing to obtain observables suitable for conductivity modelling. The second step is modelling these observables to recover the 3-D conductivity structure. The approach is tested on synthetic magnetic data from [4].

THE NUMERICAL MODEL

The mantle is divided into spherical shells. The conductivity in each shell may be uniform or it may vary horizontally, but it may not vary radially. The stack of shells starts from a homogeneous core of finite conductivity and ends at an upper boundary above which the medium is insulating. A generic earth model is shown in Fig. 1. Under the quasi-static approximation, the governing equations in the core are:

$$\begin{aligned}\nabla \cdot \mathbf{B}(\mathbf{r}, \mathbf{t}) &= 0 \\ \nabla \times \mathbf{E}(\mathbf{r}, \mathbf{t}) &= -\frac{\partial}{\partial t} \mathbf{B}(\mathbf{r}, \mathbf{t}) \\ \nabla \times \mathbf{B}(\mathbf{r}, \mathbf{t}) &= \mu \sigma_c \mathbf{E}(\mathbf{r}, \mathbf{t})\end{aligned}\tag{1}$$

where μ is the magnetic permeability in vacuum, σ_c is the constant core conductivity, and \mathbf{B} and \mathbf{E} are the total magnetic and electric fields. In the mantle the electromagnetic field satisfies:

$$\begin{aligned}\nabla \cdot \mathbf{B}(\mathbf{r}, \mathbf{t}) &= 0 \\ \nabla \times \mathbf{E}(\mathbf{r}, \mathbf{t}) &= -\frac{\partial}{\partial t} \mathbf{B}(\mathbf{r}, \mathbf{t}) \\ \nabla \times \mathbf{B}(\mathbf{r}, \mathbf{t}) &= \mu \sigma_m(\mathbf{r}) \mathbf{E}(\mathbf{r}, \mathbf{t})\end{aligned}\tag{2}$$

where the mantle conductivity $\sigma_m(\mathbf{r})$ depends on the position vector \mathbf{r} . Continuity conditions (see below) at the inner mantle boundary (IMB) relate \mathbf{E} and \mathbf{B} in the mantle just above the IMB to \mathbf{E} and \mathbf{B} in the core just below the IMB.

The time-varying part of the electric and magnetic (EM) fields are defined as $\mathbf{e}(\mathbf{r}, \mathbf{t})$ and $\mathbf{b}(\mathbf{r}, \mathbf{t})$ respectively, so that $\mathbf{B}(\mathbf{r}, \mathbf{t}) = \mathbf{B}_s(\mathbf{r}) + \mathbf{b}(\mathbf{r}, \mathbf{t})$ and $\mathbf{E}(\mathbf{r}, \mathbf{t}) = \mathbf{E}_s(\mathbf{r}) + \mathbf{e}(\mathbf{r}, \mathbf{t})$. The subscript s stands for static. The fields $\mathbf{e}(\mathbf{r}, \mathbf{t})$ and $\mathbf{b}(\mathbf{r}, \mathbf{t})$ satisfy:

$$\begin{aligned}\nabla \times \mathbf{e}(\mathbf{r}, \mathbf{t}) &= -\frac{\partial}{\partial t} \mathbf{b}(\mathbf{r}, \mathbf{t}) \\ \nabla \times \mathbf{b}(\mathbf{r}, \mathbf{t}) &= \mu \sigma_c \mathbf{e}(\mathbf{r}, \mathbf{t})\end{aligned}\tag{3}$$

below IMB while above, they satisfy:

$$\begin{aligned}\nabla \times \mathbf{e}(\mathbf{r}, \mathbf{t}) &= -\frac{\partial}{\partial t} \mathbf{b}(\mathbf{r}, \mathbf{t}) \\ \nabla \times \mathbf{b}(\mathbf{r}, \mathbf{t}) &= \mu \sigma_m(\mathbf{r}) \mathbf{e}(\mathbf{r}, \mathbf{t})\end{aligned}\tag{4}$$

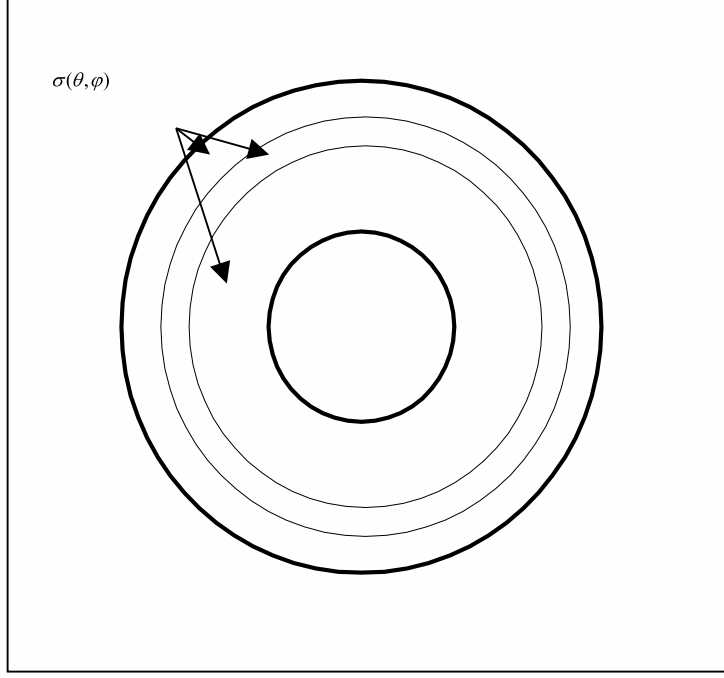


Figure 1: Spherical model.

Above the upper boundary of the conductivity layer, where the medium is assumed to be insulating, eq (4) is still valid with $\sigma_m = 0$.

The second equation in both eq (3) and eq (4) (Faraday's Law) implies that $\partial(\nabla \bullet \mathbf{b})/\partial t = \mathbf{0}$. Since \mathbf{b} is the time-dependent part of the field, this can be integrated to give $\nabla \bullet \mathbf{b} = \mathbf{0}$. Thus, the first equation in eq (1) and eq (2) is redundant and was not repeated in eq (3) and eq (4).

The boundary conditions are that all components of \mathbf{b} , the tangential components of \mathbf{e} , and the radial component of the current $\mathbf{J} = \sigma \mathbf{e}$, are continuous across the IMB, across the upper boundary of the conductivity layer in the mantle, and across every internal boundary separating two adjacent shells in the conductive mantle. One consequence of these boundary conditions is that the radial component of \mathbf{e} must vanish at the upper boundary of the conductivity layer since $\sigma = 0$ above that boundary.

The solution to equations (3) and (4) is written as:

$$\begin{aligned} \mathbf{e}(\mathbf{r}, \mathbf{t}) &= \mathbf{e}_n(\mathbf{r}, \mathbf{t}) + \mathbf{e}_a(\mathbf{r}, \mathbf{t}) \\ \mathbf{b}(\mathbf{r}, \mathbf{t}) &= \mathbf{b}_n(\mathbf{r}, \mathbf{t}) + \mathbf{b}_a(\mathbf{r}, \mathbf{t}) \end{aligned} \quad (5)$$

where the normal field, $(\mathbf{e}_n, \mathbf{b}_n)$, is the solution for a homogeneous core ($\sigma = \sigma_c$) and an insulating mantle ($\sigma = 0$). The anomalous field, $(\mathbf{e}_a, \mathbf{b}_a)$ represents the effects of mantle conductivity. The equations which govern the normal field $\mathbf{e}_n(\mathbf{r}, \mathbf{t})$ and $\mathbf{b}_n(\mathbf{r}, \mathbf{t})$ are:

$$\left. \begin{aligned} \nabla \times \mathbf{e}_n(\mathbf{r}, \mathbf{t}) &= -\frac{\partial}{\partial t} \mathbf{b}_n(\mathbf{r}, \mathbf{t}) \\ \nabla \times \mathbf{b}_n(\mathbf{r}, \mathbf{t}) &= \mu \sigma_c \mathbf{e}_n(\mathbf{r}, \mathbf{t}) \end{aligned} \right\} \text{in the core} \quad (6)$$

$$\left. \begin{aligned} \nabla \times \mathbf{e}_n(\mathbf{r}, \mathbf{t}) &= -\frac{\partial}{\partial t} \mathbf{b}_n(\mathbf{r}, \mathbf{t}) \\ \nabla \times \mathbf{b}_n(\mathbf{r}, \mathbf{t}) &= 0 \end{aligned} \right\} \text{above the core} \quad (7)$$

The field \mathbf{b}_n , the horizontal components of \mathbf{e}_n , and the radial component of the electric current $\mathbf{J}_n = \sigma \mathbf{e}_n$ are all continuous across the IMB. Hence $\sigma_c e_{nr} = J_{nr} = 0$ at the core side of the IMB, since for the normal field the medium above the IMB is assumed to be insulating. As a consequence, e_{nr} at the IMB (core side) is null. Subtracting eq. (6) from (1) and (7) from (2), we obtain the set of equations for the anomalous field:

$$\left. \begin{aligned} \nabla \times \mathbf{e}_a(\mathbf{r}, \mathbf{t}) &= -\frac{\partial}{\partial t} \mathbf{b}_a(\mathbf{r}, \mathbf{t}) \\ \nabla \times \mathbf{b}_a(\mathbf{r}, \mathbf{t}) &= \mu \sigma_c \mathbf{e}_a(\mathbf{r}, \mathbf{t}) \end{aligned} \right\} \text{in the core} \quad (8)$$

$$\left. \begin{aligned} \nabla \times \mathbf{e}_a(\mathbf{r}, \mathbf{t}) &= -\frac{\partial}{\partial t} \mathbf{b}_a(\mathbf{r}, \mathbf{t}) \\ \nabla \times \mathbf{b}_a(\mathbf{r}, \mathbf{t}) - \mu\sigma_m(\mathbf{r})\mathbf{e}_a(\mathbf{r}, \mathbf{t}) &= \mu\sigma_m(\mathbf{r})\mathbf{e}_n(\mathbf{r}, \mathbf{t}) \end{aligned} \right\} \text{in the mantle} \quad (9)$$

The magnetic field \mathbf{b}_a and the horizontal components of the electric field \mathbf{e}_a are continuous across all boundaries. The boundary condition on the radial component of the anomalous current, $\mathbf{J}_a = \sigma\mathbf{e}_a$, is more complicated, and is determined by the requirement that the total, time-variable, radial current, $\sigma(\mathbf{e}_n + \mathbf{e}_a)$ be continuous across each boundary. At any boundary in the mantle, the conditions is:

$$\sigma(\mathbf{r}^-)\mathbf{e}_{ar}(\mathbf{r}^-, \mathbf{t}) - \sigma(\mathbf{r}^+)\mathbf{e}_{ar}(\mathbf{r}^+, \mathbf{t}) = \sigma(\mathbf{r}^+)\mathbf{e}_{nr}(\mathbf{r}^+, \mathbf{t}) - \sigma(\mathbf{r}^-)\mathbf{e}_{nr}(\mathbf{r}^-, \mathbf{t}) \quad (10)$$

where the superscripts + and - refer to just above and just below the boundary. Equation (10) also describes the continuity of e_{ar} at the IMB (where $e_{nr}(\mathbf{r}^-, \mathbf{t}) = \mathbf{0}$); and at the upper boundary of the conductive region in the mantle (where $\sigma = 0$).

This separation of the field into normal and anomalous components allows us to solve the problem in two steps. First, eqs (6-7) are solved to obtain the normal field. We then use this normal field as the source term for generating the anomalous field, using the \mathbf{e}_n terms in eqs (9-10). We define the current source in terms of the electric and magnetic fields it would produce in an earth with a spherical homogeneous core and an insulating mantle. Hence we simply assume the normal field is known throughout the mantle, and we use that field in eqs (9-10). We do ensure that this known normal field is consistent with eq. (7) in the mantle.

The fact that the boundaries in our earth model are all spherical surfaces, means that our equations can be solved most easily in spherical coordinates, (r, θ, φ) , where θ and φ are the colatitude and eastward longitude respectively. Although the laterally-varying conductivity removes spherical symmetry, it is useful to employ spherical harmonic expansions when solving the equations. Accordingly, the electric and magnetic fields are expanded into a generalized spherical harmonics (GSH) series Y_l^{Nm} using the canonical basis $(\hat{\mathbf{e}}^+, \hat{\mathbf{e}}^0, \hat{\mathbf{e}}^-)$. In this basis, a vector \mathbf{F} has the form:

$$\mathbf{F}(\mathbf{r}, \theta, \varphi) = \sum^N \mathbf{F}^N(\mathbf{r}, \theta, \varphi)\hat{\mathbf{e}}^N = \sum_{N,l,m} \mathbf{F}_l^{Nm}(\mathbf{r})\mathbf{Y}_l^{Nm}(\theta, \varphi)\hat{\mathbf{e}}^N \quad N=-1,0,+1 \quad (11)$$

The $N = 0$ terms in eq. (11) describe the radial component of \mathbf{F} . The horizontal components F_l^{+1m} and F_l^{-1m} are combined into toroidal and spheroidal (or poloidal) component, F_l^{Tm} and F_l^{Pm} respectively.

The GSH expansions of the \mathbf{e} and \mathbf{b} fields in eqs (6-10) are used to obtain differential equations for the GSH coefficients in these expansions. The equations are solved in the frequency domain, assuming a time dependence of $e^{i\omega t}$ for \mathbf{e} and \mathbf{b} where ω is the angular frequency. The resulting equations are first order ordinary differential equations in the radial coordinate r .

Solution for the normal field

The normal field can be completely determined in the mantle by specifying the values of the spherical harmonic components of the radial magnetic and electric field at the IMB (mantle side, $r = c^+$), $b_{nl}^{0m}(c^+)$ and $e_{nl}^{0m}(c^+)$, for every spherical harmonic degree and order (l, m) . The continuation of these IMB values up through the insulating mantle can be determined from the GSH expansion of eq (6-7). For the b_{nl}^{0m} case the solution for the normal EM field in the insulating mantle is:

$$\left[\begin{array}{c} b_{nl}^{Pm}(r) \\ b_{nl}^{0m}(r) \end{array} \right] = b_{nl}^{0m}(c^+) \left(\frac{c}{r}\right)^{l+2} \left[\begin{array}{c} -l \\ 1 \end{array} \right] \quad (12)$$

$$e_{nl}^{Tm}(r) = \omega r b_{nl}^{0m}(c^+) \left(\frac{c}{r}\right)^{l+2}$$

$$e_{nl}^{Pm}(r) = e_{nl}^{0m}(r) = b_{nl}^{Tm}(r) = 0$$

For the e_{nl}^{0m} case, the solution is:

$$\left[\begin{array}{c} e_{nl}^{Pm}(r) \\ e_{nl}^{0m}(r) \end{array} \right] = e_{nl}^{0m}(c^+) \left(\frac{c}{r}\right)^{l+2} \left[\begin{array}{c} -l \\ 1 \end{array} \right] \quad (13)$$

$$e_{nl}^{Tm}(r) = b_{nl}^{0m}(r) = b_{nl}^{Pm}(r) = b_{nl}^{Tm}(r) = 0$$

Solution for the anomalous field

In the mantle, eqs (2) are expanded into GSH. The resulting equations for the anomalous field are obtained from the GSH expansion of eq. (9). For each degree and order (l, m), the following first order system of differential equations is obtained:

$$\frac{d}{dr} \begin{bmatrix} b_{al}^{Pm} \\ b_{al}^{0m} \\ e_{al}^{Pm} \\ J_{al}^{0m} \end{bmatrix} - \begin{bmatrix} -\frac{1}{r} & \frac{2\Omega_l}{r} & 0 & 0 \\ \frac{1}{r} & -\frac{2}{r} & 0 & 0 \\ 0 & 0 & -\frac{1}{r} & i\omega\mu r \\ 0 & 0 & 0 & -\frac{2}{r} \end{bmatrix} \begin{bmatrix} b_{al}^{Pm} \\ b_{al}^{0m} \\ e_{al}^{Pm} \\ J_{al}^{0m} \end{bmatrix} - \begin{bmatrix} i\mu J_{al}^{Tm} \\ 0 \\ \frac{2\Omega_l}{r} e_{al}^{0m} \\ \frac{1}{r} J_{al}^{Pm} \end{bmatrix} = \begin{bmatrix} i\mu J_{nl}^{Tm} \\ 0 \\ i\omega\mu r J_{nl}^{0m} \\ -\frac{2}{r} J_{nl}^{0m} - \frac{d}{dr} J_{nl}^{0m} + \frac{1}{r} J_{nl}^{Pm} \end{bmatrix} \quad (14)$$

where $J_{nl}^{0m}, J_{nl}^{Pm}, J_{nl}^{Tm}$ are the radial, poloidal, and toroidal (l, m) GSH components of the electric current $\sigma(\mathbf{r})\mathbf{e}_n(\mathbf{r}, \omega)$; and $J_{al}^{0m}, J_{al}^{Pm}, J_{al}^{Tm}$ are the radial, poloidal, and toroidal (l, m) GSH components of the electric current $\sigma(\mathbf{r})\mathbf{e}_a(\mathbf{r}, \omega)$.

The system (14) is described as follows: the anomalous \mathbf{e} and \mathbf{b} fields are represented by the four functions of radius $[b_{al}^{Pm}(r), b_{al}^{0m}(r), e_{al}^{Pm}(r), J_{al}^{0m}(r)]$ for each (l, m). The anomalous current J_{al}^{0m} is used instead of e_{al}^{0m} because it simplifies the mathematics. These four functions are represented with the symbol:

$$Z^{lm}(r) = [b_{al}^{Pm}(r), b_{al}^{0m}(r), e_{al}^{Pm}(r), J_{al}^{0m}(r)] \quad (15)$$

To completely describe the \mathbf{e} and \mathbf{b} fields, the toroidal components b_{al}^{Tm} and e_{al}^{Tm} need to be specified. But those components are related to the other four variables through simple algebraic relations that do not involve radial differentiation. The system (14) thus, can be considered as a forced ordinary differential equation for the anomalous \mathbf{e} and \mathbf{b} fields, with the unknown scalars on the left-hand side and the forcing from the known normal field on the right-hand side.

The last term on the left-hand-side of (14) includes the scalars J_{al}^{Tm}, e_{al}^{0m} and J_{al}^{Pm} which are not among the four components used to describe the anomalous fields. These three scalars, however, can be directly related to our four components. For example, e_{al}^{0m} is the (l, m) component in the Y_l^{Nm} expansion of:

$$J_{al}^0(r, \theta, \varphi) / \sigma(r, \theta, \varphi) = \left[\sum_{l', m'} J_{al'}^{0m'}(r) Y_{l'}^{0m'}(\theta, \varphi) \right] / \sigma(r, \theta, \varphi) \quad (16)$$

In this way $e_{al}^{0m}(r)$ can be related to the $\{J_{al'}^{0m'}(r)\}$. For laterally-varying conductivity, e_{al}^{0m} will, in general, depend on all the $J_{al'}^{0m'}$ (ie on $J_{al'}^{0m'}$ with $l, m \neq l', m'$). Similar results hold for $J_{al}^{Tm}(r)$ and $J_{al}^{Pm}(r)$. Thus, the last term on the left-hand-side of (14) is viewed as a direct, though complicated, linear function of the $\{Z^{l'm'}\}$.

Numerical considerations

In an heterogeneous shell (Fig. 1), the system (14) is integrated upward from the bottom of the shell to its top with a fourth-order Runge Kutta integration technique though when a shell is homogeneous, we use instead an analytical solution to eqs (14). To improve the accuracy, the shell may be subdivided into thinner shells according to a criteria based upon the minimum penetration depth in the shell. The maximum thickness across which the system of eqs (14) is numerically integrated should not exceed a fraction of the minimum penetration depth (penetration depth = $\sqrt{2/\omega\mu\sigma_{max}}$). We found that a fraction equal to 0.4 was a good compromise between the numerical accuracy for the integration and the necessity to limit the number of subdivisions to minimise the computation time..

Propagation across boundaries is done in a similar manner. The fields just below the boundary between two adjacent shells are converted back to the spatial domain, and multiplied by the conductivity when appropriate. The fields just above are obtained using the boundary conditions and then are expanded again into GSH and propagated through the next shell.

INVERSION

The inversion is based on the minimisation of a misfit function between observables and a model. The magnetic potential E (external) and I (internal) coefficients could be used as such. However, they contain noise and some statistical estimates should be determined. In order to optimize the signal over noise ratio, the following

procedure is proposed. Time windows of given lengths (say 30 or 60 days) are selected and the E and I coefficients are obtained for each time window. For $lmax_0(lmax_0 + 2)$ external source coefficients, each internal coefficients of degree and order l, m is given by:

$$I_l^{0m}(\omega, n) = \sum_{l_0, m_0} Q_{lm}^{l_0 m_0}(\omega) E_{l_0}^{0m_0}(\omega, n) \quad (17)$$

where n is the window number and Q the induced response function of degree and order l, m forced by a unit source term of degree and order l_0, m_0 . We defined the internal vs external co- and cross-spectra as:

$$\begin{aligned} S_{ee}^{lm, l_0 m_0}(\omega) &= \frac{1}{NW} \sum_n E_l^{0m}(\omega, n) (E_{l_0}^{0m_0}(\omega, n))^* \\ S_{ie}^{lm, l_0 m_0}(\omega) &= \frac{1}{NW} \sum_n I_l^{0m}(\omega, n) (E_{l_0}^{0m_0}(\omega, n))^* \end{aligned} \quad (18)$$

where NW is the number of time windows. Various trials were carried out using 1-3 satellites, 1-3 years of data and 30 or 60 days windows. The maximum degree for the external field was 3 and 7-9 for the internal field. The periods in days range from 2 to TW days where TW is the window length.

The 3-D modelling of the electrical conductivity in the earth at the global scale implies the use of a 3-D spherical solver. Reference [4] generated the synthetic satellite data using the forward code proposed by [5]. In order to perform an inversion of these data, it is best to use a forward solver entirely different. The one used here [6,7] is based on the space/spectral approach described above. The forcing field is given by its SH coefficients and is applied at the earth surface. Since the E and I coefficients are obtained at the earth surface, there is no need to continue the computed field upward to satellite altitude. The approach proposed here to invert the satellite data is based on the modelling of potential coefficients recovered. Nevertheless the data analysis involved to obtain these coefficients may only provide a limited number of SH coefficients at a limited number of periods. The question therefore is whether or not such restricted number of coefficients carries enough information to recover the conductivity structure with a reasonable degree of accuracy.

The strategy proposed here is to run the inversion to find a model that fit the S_{ie} values given the S_{ee} . In standard magnetotelluric or global induction analysis, 1-2 source terms are considered and the Q values (or functions of the Q values) are uniquely obtained from eq. 18 or equivalent relationships. Here, the approach is more general. There may be an unknown number of time-independant source terms. They may have different geometries and similar time dependency. As a result, the Q values cannot be uniquely obtained (although the $l = 1, m = 0$ term is always dominant and well characterized).

The first step is to calculate the Q values (eq. 17) for all l_0, m_0 values of the source field. Then the theoretical co-spectrum $S_{ie}(cal)$ is obtained from the combination of the calculated Q values and the observed external E coefficients using eqs. 17-18. The misfit function used in the inversion procedure is defined as follow:

$$\chi^2 = \sum_{\omega, l, m, l_0, m_0} \left[S_{ie}^{lm, l_0 m_0}(\omega)_{obs} - S_{ie}^{lm, l_0 m_0}(\omega)_{cal} \right]^2 W^{lm, l_0 m_0}(\omega) + \lambda \sum_{i, j}^{\sigma} [\log(\sigma_i / \sigma_j)]^2 \quad (19)$$

The misfit is weighte with the coefficient W . The second term on the right hand side of eq. 19 is the smoothness term which minimizes the log-conductivity differences between all meshes in a layer and the mean log-conductivity value between layers.

In the inverse procedure, the starting model is 1-D and is the best 1-D fitting model obtained using the coefficients E and I up to $l = 3$. The 3-D solver was used for the inversion but with homogeneous layers. Fig. 2 shows the best fitting 1-D model compared to the mantle structure used in conductivity models of type I to generate the data.

Before running the full 3-D inversion to recover the mantle structure, it is necessary to deal with the uppermost crustal structures, namely the distribution of oceanic masses and large sedimentary basins responsible for large distorsion of the induced geomagnetic field.

Accounting for the coast effect

The coast effect is the generic name to describe the electromagnetic distorsion caused by the large conductivity contrast between oceanic or sedimentary basins and the electrically resistive bedrock. Here we proposed to generalize the approach proposed by [8] to include the coast effect in the inversion procedure.

Following reference [4], we define a model comprise of the 1-D conductivity structure topped by an heterogeneous sheet of conductance $\tau = \tau_n + \tau_a$ where τ_n is the conductance of the ocean (see ref. [4]). We define a

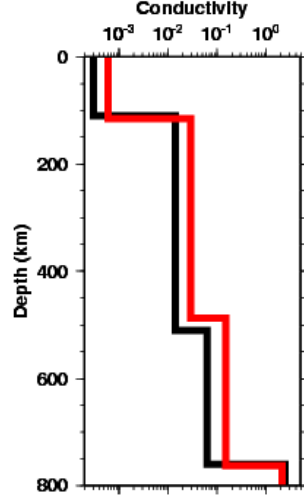


Figure 2: Best fitting 1-D model (in red) for the minimum misfit function between the FSHE internal coefficients I . The original 1-D structure beneath the heterogeneous upper shell used to synthesize the data is in black.

new normal model which is the 1-D conductivity structure topped by a uniform sheet of conductance τ_n . The corresponding total horizontal normal field at the earth surface is \mathbf{E}_{ns} . The total horizontal electric field \mathbf{E}_s at a given position \mathbf{r}_0 at the earth surface is solution of an integral equation of the type:

$$\mathbf{E}_s(\mathbf{r}_0) = \mathbf{E}_{ns}(\mathbf{r}_0) + \int_{\partial V_a} \tau_a(\mathbf{r}) \mathbf{G}_s(\mathbf{r}_0, \mathbf{r}) \mathbf{E}_s(\mathbf{r}) d\mathbf{s} \quad (20)$$

where \mathbf{G}_s is the surface Green dyadic and ∂V_a the anomalous domain (compared to the normal model with the top layer of conductance τ_n). Now we introduce an anomalous body in the mantle of conductivity $\sigma = \sigma_n + \sigma_a$. The surface electric field becomes:

$$\mathbf{E}_s(\mathbf{r}_0) = \mathbf{E}_{ns}(\mathbf{r}_0) + \int_{\partial V_a} \tau_a(\mathbf{r}) \mathbf{G}_{s1}(\mathbf{r}_0, \mathbf{r}) \mathbf{E}_{s1}(\mathbf{r}) d\mathbf{s} + \int_{V_a} \sigma_a(\mathbf{r}) \mathbf{G}_{s2}(\mathbf{r}_0, \mathbf{r}) \mathbf{E}_2(\mathbf{r}) d\mathbf{v} \quad (21)$$

where the subscripts 1 and 2 correspond to the top sheet and the mantle anomalous body respectively. We note \mathbf{E}_{Ms} the surface electric field for a model with a normal surface sheet (of conductance τ_n and the anomalous mantle body). This field is solution of:

$$\mathbf{E}_{Ms}(\mathbf{r}_0) = \mathbf{E}_{ns}(\mathbf{r}_0) + \int_{V_a} \sigma_a(\mathbf{r}) \mathbf{G}_{s2}(\mathbf{r}_0, \mathbf{r}) \mathbf{E}_2(\mathbf{r}) d\mathbf{v} \quad (22)$$

The general solution of eq. 20 is of the form:

$$\mathbf{E}_s(\mathbf{r}_0) = \mathbf{E}_{ns}(\mathbf{r}_0) + \int_{\partial V_a} \mathbf{K}_s(\mathbf{r}_0, \mathbf{r}) \mathbf{E}_{ns}(\mathbf{r}) d\mathbf{s} \quad (23)$$

where \mathbf{K} is a kernel function of both the normal model and the anomalous domain. At the long period considered here (more than 1 day), the mutual induction of the anomalous electric currents distorted by the surface and deep heterogeneities is weak and may be neglected [8-9]. Within the approximation that mutual coupling between anomalous currents flowing in domains (1) and (2) is negligible, the solution of eq. 21 at earth surface is of the form:

$$\mathbf{E}_s(\mathbf{r}_0) = \mathbf{E}_{Ms}(\mathbf{r}_0) + \int_{\partial V_a} \mathbf{K}_s(\mathbf{r}_0, \mathbf{r}) \mathbf{E}_{Ms}(\mathbf{r}) d\mathbf{s} \quad (24)$$

The mantle field \mathbf{E}_M plays the role of the normal field with the same distortion kernel \mathbf{K} as in eq. 23. Hence, the kernel \mathbf{K} may be calculated for the normal model from eq. 23 and included into eq. 24 to account for the distortion of the mantle field \mathbf{E}_M by the surface heterogeneous layer.

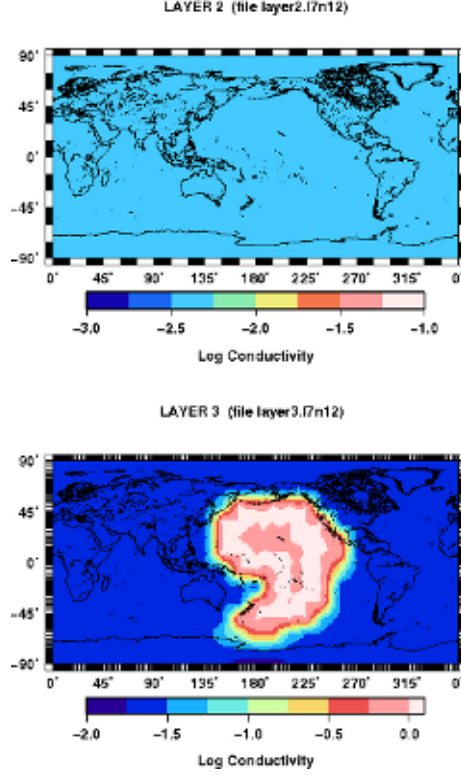


Figure 3: result of the 3-D inversion obtained from the synthetic E and I coefficients [4]. The color scale is the log of the electrical conductivity.

Calculation of the distortion kernels \mathbf{K}

It is convenient to consider the SHE of eq. 23 in order to determine the distortion coefficients of the kernel \mathbf{K} . Using a generalized SH approach, we define the toroidal electric field at the earth surface $E_V^{Tm'}$ of the distorted field and E_{nl}^{Tm} of the normal field. After some algebra, the SHE of eq. 24 is obtained and may be written as:

$$E_V^{Tm'} = E_{nl}^{Tm} \delta_{lm}^{l'm'} + K_{lm}^{l'm'} E_{nl}^{Tm} \quad (25)$$

where δ is the Kronecker symbol and the K values are the SHE coefficients of the distortion.

The forward calculation for the normal model topped by the heterogeneous sheet for all possible forcing terms l', m' provides all necessary K values. In order to accurately calculate these coefficients, the surface structure must be well described. Here we used a maximum SHE degree of 27. In order to obtain the distortion coefficients for all SHE values of the mantle field (of maximum degree l_M , the forward calculation must be carried out $l_M(l_M + 2)$ times for each period which may be a lot. However it is done once.

The distorted mantle field observed at the earth surface is a function of the internal and external coefficients. The value E_{MT} is calculated as follow:

$$E_V^{Tm'} = E_{Ml}^{Tm} \delta_{lm}^{l'm'} + K_{lm}^{l'm'} E_{Ml}^{Tm} \quad (26)$$

it is straightforward to obtain (using A15) the internal potential Q_M of degree and order l, m for a unit external forcing of degree and order l_0, m_0 . These values for all necessary internal and external degrees and orders are combined with the observed external field in eq. 18 to obtain the calculated cross-spectrum $S_{ie}(cal)$ in eq. 19.

Results of the 3D inversion

The inversion started with the 1-D model in Figure 2. The non-linear minimisation of the misfit function (19) varies successively the conductivity in all meshes in the layers ascribed to be heterogeneous (namely layers 2 and 3). The top layer is homogeneous and of conductivity 3.2 S/m. At each iteration, the mantle Q coefficients

are calculated and corrected for coast effect using eq. 26 from which we derive the distorted Q values. The misfit is then calculated according to eq. 19.

The minimisation procedure starts with no or very little smoothness. Then the smoothness is added. The coefficient λ in eq. 19 is adjusted so that the smoothness is of same order as the misfit. The minimisation is stopped when the misfit starts to increase while the smoothness is decreasing.

In figure 3, we present the inversion result using the exact time series I and E coefficients used by ref [5] to generate the E2E magnetospheric (external+induced) data. In this example, the maximum degree of the internal SHE is 9. The time series of the coefficients were Fourier transformed by time windows of 30 days over 1 year. The Fourier coefficients were combined to form the co- and cross-spectra values S_{ie} and S_{ee} used to build the misfit function (19). The grid is divided into 12x24 cells. The structure is correctly recovered. The various tests carried out showed the importance of a priori information about the radial layering, here provided by the prior 1-D analysis. The smoothness criteria proved to be efficient to remove spurious effect in layer 2 but removed also any features related to the structures in that layer, however too small to be retrieve with the spatial resolution used here.

CONCLUSION

A general approach was proposed to process and invert satellite geomagnetic data to infer the 3-D conductivity of the earth. Both data analysis and inversion scheme were proved satisfactory to process synthetic data. While the approach presented here seems to work reasonably well, it is only a partial answer to the question of magnetic data inversion for induction studies. A simple case with a pure magnetospheric source was considered. The inverse solution was found for satellite data synthesized with conductivity models with the mantle structures. At the resolution used here (18x18 or 12x12 degrees grid), only the major features were recovered.

REFERENCES

- [1] Olsen, N., Induction studies with satellite data, *Surveys in Geophysics*, 20, 309-340, 1999.
- [2] Tarits P., Preliminary investigation of the oersted data for induction studies, Oersted 3rd international Science team meeting, proceedings, 2000
- [3] Constable S. and C. Constable, Observing geomagnetic induction in magnetic satellite measurements and associated implications for mantle conductivity, *Geochemistry, Geophysics, Geosystems*, 5, doi:10.1029/2003GC000,634, 2004.
- [4] Kuvshinov A, T. Sabaka, and N. Olsen, 3-D electromagnetic induction studies using the Swarm constellation: Mapping conductivity anomalies in the Earth's mantle *Earth Planets Space*, 58, 417-427, 2006.
- [5] Kuvshinov, A. V., D. B. Avdeev, O. V. Pankratov, S. A. Golyshev, and N. Olsen, Modelling electromagnetic fields in 3D spherical Earth using fast integral equation approach, in *3D Electromagnetics*, edited by M. S. Zhdanov and P. E. Wannamaker, chap. 3, pp. 43-54, Elsevier, Holland, 2002.
- [6] Tarits P., J. Wahr and P. Lognonn, Influence of conductivity heterogeneities at and near the CMB on the geomagnetic secular variation, AGU Fall meeting, 1998.
- [7] Grammatika N. and P. Tarits, Contribution at satellite altitude of electromagnetically induced anomalies from a 3-D heterogeneously conducting earth, *Geophys. J. Int.*, 151, 3, 913-923., 2002
- [8] Nolasco R., P. Tarits, J.H. Filloux, and A.D. Chave, Magnetotelluric imaging of the Tahiti Hot Spot, *Journal of Geophysical Research*, 103, pp 30,287-30,309. 1998
- [9] Tarits P. and M. Menvielle M., Study of an anomalous magnetic-field of intralithospheric origin; *Can. J. Earth Sci.* 1983, Vol 20, Iss 4, pp 537-547